Determination of Differential Mobility Analyzer Transfer Functions Using Identical Instruments in Series

W. Birmili, F. Stratmann, A. Wiedensohler, D. Covert, L. M. Russell, and O. Berg*

INSTITUTE FOR TROPOSPHERIC RESEARCH, PERMOSERSTR. 15D-04303 LEIPZIG, GERMANY (W. B., F. S., A. W.); DEPARTMENT OF ATMOSPHERIC SCIENCES, UNIVERSITY OF WASHINGTON, SEATTLE, WA 98195, USA (D. C.); DEPARTMENT OF CHEMICAL ENGINEERING, CALIFORNIA INSTITUTE OF TECHNOLOGY, PASADENA, CA 91125, USA (L. M.); DEPARTMENT OF NUCLEAR PHYSICS, LUND UNIVERSITY, S-23362 LUND, SWEDEN (O. B.)

ABSTRACT. The differential mobility analyzer (DMA) is an important tool for determining particle size distributions. The physical performance of a DMA is quantified by the concept of the transfer function. Therefore, knowledge of the transfer function is important to interpret the mobility distributions recorded by a DMA.

During a calibration workshop in preparation for the Aerosol Characterization Experiment 1 (ACE1) field campaign, the transfer functions of five types of different mobility analyzers (Vienna-type DMA short, medium, and long, CIT radial, and TSI long; CIT = California Institute of Technology, Pasadena, CA; TST = TSI Inc., St. Paul, MN) were experimentally characterized by height, width, and area of their transfer functions. Different particles size ranges between 3 and 200 nm were investigated.

The transfer function was determined by scanning a DMA across the mobility distribution produced by another, identical DMA. Subsequently, the data were processed by a deconvolution algorithm assuming a triangular shape for the transfer function. For all DMA types, the area of the transfer function decreased with particle size, especially for ultrafine particles ($d_p < 20$ nm). The gradient with which this area decreases with particle size, however, is different for each of the DMA types investigated. The calibration provides an improved description of the performance of each DMA, particularly in the ultrafine size range. AEROSOL SCIENCE AND TECHNOLOGY 27:215–223 (1997)

1. INTRODUCTION

The differential mobility analyzer (DMA) is an important tool for measuring particle size distributions. The concept of the transfer function quantifies the physical performance of a DMA which is important to interpret, or "invert" the mobility distributions recorded by a DMA. Stratmann et al. (1996) show that recalculated size distributions are improved when utilizing a more accurate, size-dependent transfer function for the data inversion. Especially, the number of ultrafine particles ($d_p < 20$ nm) can

* Corresponding author.

Aerosol Science and Technology 27:215–223 (1997)

Published by Elsevier Science Inc.

0278-6826/97/$17.00
PII S0278-6826(97)00009-3

TABLE 1. Technical Reference for the DMA Types Used in this Work[a]

DMA Type	Reference	Geometric Parameters			Operation Parameters as Used in this Experiment	
		L (cm)	r_i (mm)	r_a (mm)	Flow Ratio (1/min)	Diameter Range (nm)
(a) Vienna-type (short)	Winkelmayr et al. (1991)[b]	11.0	25.0	33.5	2.0/20	3.5–65
(b) CIT Radial	Zhang et al. (1995)	—[c]	—[c]	—[c]	0.5/5.0	8.0–75
(c) Vienna-type (medium)	Winkelmayr et al. (1991)[b]	28.0	25.0	33.5	0.5/5.0	15–100
(d) TSI Long	Model 3071a, TSI, St. Paul, MN	44.4	9.37	19.58	1.0/5.0	13–100
(e) Vienna-type (long)	Winkelmayr et al. (1991)[b]	50.0	25.0	33.5	1.0/10	35–200

[a] Nomenclature: L = distance between the mobility analyzer entrance slit and sampling slit; r_i = radius of the center (inner) electrode; r_a = radius of the housing (outer electrode).

[b] The Vienna-type DMAs (a), (c), and (e) follow the design presented in Winkelmayr et al. (1991, DMA type 3/150, Fig. 1) with variances in the exact dimensions used.

[c] For the CIT radial, different geometric parameters are relevant (for details, see reference): b (=distance between parallel electrode plates) = 1.0 cm; R_1 (=radius of aerosol outlet tube) = 2.4 mm; R_2 (=radial distance of the aerosol inlet from the DMA's axis) = 50.4 mm.

thus be better estimated. In this size range, the DMA deviates significantly from its theoretically derived transfer functions (Kousaka et al., 1985; Zhang et al., 1995; Fissan et al., 1996). Two principal effects of Brownian diffusion are thought to be responsible for degrading the transfer function: First, particle losses in connecting tubings and inlets of the DMA (decreases the area of the transfer function) and second, broadening of particle trajectories inside the analyzer column (increases the width of the transfer function) which can be described according to Stolzenburg (1988). Also the shape of the transfer function is altered.

The aim of this work was to determine the transfer functions of five different types of DMAs as a function of particle size. The DMA types investigated are Vienna short, medium, and long, CIT radial, and TSI long. Table 1 provides detailed physical specifications for each DMA. All five DMAs will be used for particle size measurements during the ACE1[1] and ACE2[2] field campaigns. Therefore, the calibration was performed under the specific conditions (i.e., DMA flow rates and particle size range) for these operations.

2. DESCRIPTION OF THE METHOD

A schematic of the experimental setup is shown in Fig. 1. Two identical DMAs are aligned in series (tandem DMA). An aerosol generator provides particles in the diameter range 3–100 nm. Below 50 nm, a condensation type generator (Scheibel and Porstendörfer, 1983) was used to produce Ag or NaCl particles. Above 50 nm, an atomizer was operated to atomize an aqueous solution of NaCl. When using the atomizer, the wet aerosol was dried behind the generator by means of a diffusion dryer. Both DMAs and the generator were operated at atmospheric pressure.

During each measurement, the voltage of DMA-0 was held fixed at a value U_0 corresponding to the particle mobility $Z_{p,0}$ or particle diameter $d_{p,0}$ of interest. As the mobility distribution of the generator is usually much wider than the DMA transfer function, DMA-0 provides, in first approximation, a mobility distribution with the shape of the transfer function of DMA-0. The voltage U applied to DMA-1 was var-

[1] International Global Atmospheric Chemistry Project, Aerosol Characterization Experiment 1 (ACE1), held in Tasmania (Australia), 1995.

[2] Aerosol Characterization Experiment 2 (ACE2), to be held over the North Atlantic, 1997.

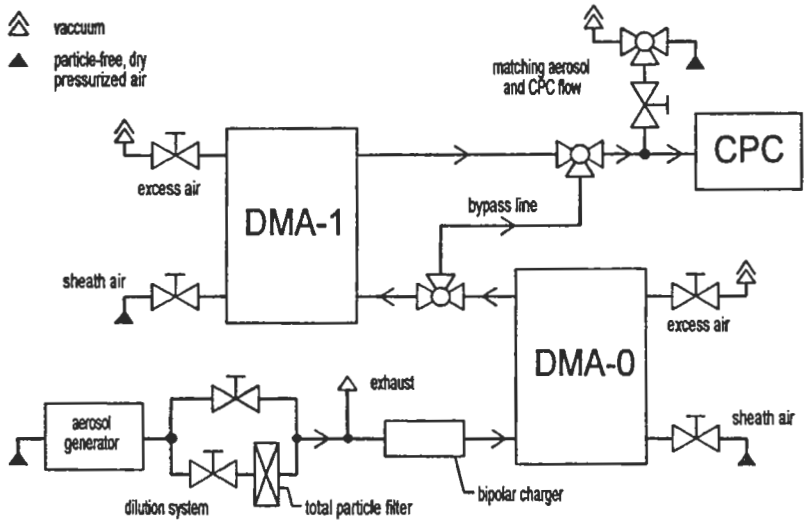

FIGURE 1. Experimental setup for determining the DMA transfer function using identical DMAs in series.

ied so that a mobility interval around the midpoint mobility $Z_{p,0}$ was scanned. U was varied exponentially and quasi-continuously (cf. Wang and Flagan, 1990). The voltage was incremented in steps as small as possible, restricted only by the resolution of the computer control card (2.44 mV). A condensation particle counter (CPC; model 3010 for $d_p > 20$ nm or model 3025A for $d_p < 20$ nm; TSI, St. Paul, MN) was used to count the particles during the scan. From these counts, the raw concentration $N'(Z_p)$ was calculated.

The particle concentrations produced by the generator may be quite high. To avoid measurement errors due to coincidence inside the CPC, a dilution system (Fig. 1) was operated downstream of the aerosol generator.

To insure that both DMAs perform equally, they were operated at the same aerosol and sheath air flow rates (listed in Table 1). The nominal CPC flow and the DMA aerosol flow were matched either by adding clean make-up air (for CPC flow > DMA flow) or removing excess aerosol (for CPC flow < DMA flow) downstream of DMA-1. All flow rates were set by using needle valves and a bubble flow meter (Gillian Corp.).

As shown in Stratmann et al. (1996), the raw data $N'(Z_p)$ must be normalized by N_0, the total aerosol concentration downstream of DMA-0:

$$N(Z_p) = N'(Z_p)/N_0.$$

N_0 was determined before and after each scan procedure by switching the flow of DMA-0 to a bypass line (Fig. 1). To insure that particle losses along both alternative pathways are equivalent, both paths were constructed so that the total length and curvature of both branches were equal. Thus, particle losses outside the DMAs cancel in the normalization procedure and, consequently, no calibration of aerosol lines for particle losses is necessary. In the context of this investigation, the boundaries of the DMAs were drawn at the inlet tubes of the classifier column. All measurements were controlled by a personal computer which included setting the DMA voltages and reading the CPC counts.

After normalizing, the tandem DMA scans were smoothed with a Fourier low-pass filter and then deconvoluted (Stratmann et al., 1996) assuming a triangular shape for the transfer function. As a result, both the height α and the half-width β of the transfer function were calculated. The algorithm utilizes a least-squares method to match experimental and calculated data.

It is assumed that both DMAs are identical with respect to α and β, and that these parameters remain constant during one scan. Precautions were taken to insure that both DMAs were identical. A visual comparison of the experimental and calculated tandem DMA scans (by shape) assures that the two DMAs have the same β. Then, α still could be different for both DMAs. This, however, was excluded by switching

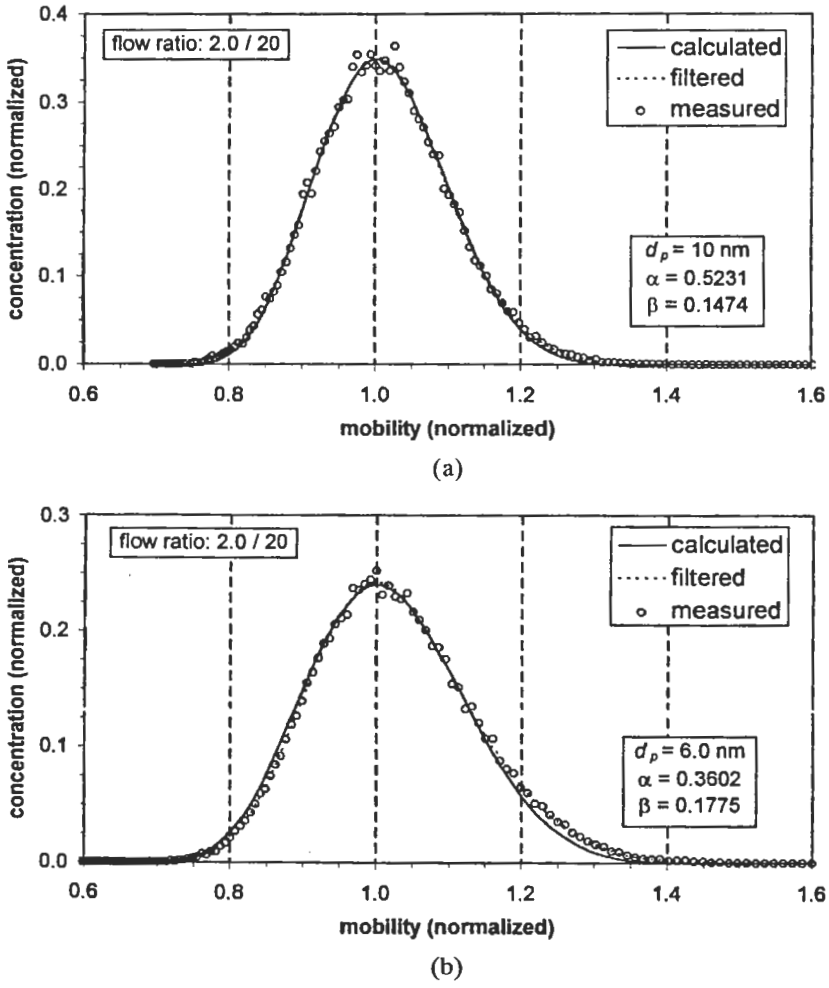

FIGURE 2. Tandem DMA scan (Vienna short) for $d_p = 10$ nm. (b) tandem DMA scan (Vienna short) for $d_p = 6.0$ nm. (c) tandem DMA scan (Vienna short) for $d_p = 3.5$ nm. (d) tandem DMA scan (CIT radial) for $d_p = 8.0$ nm.

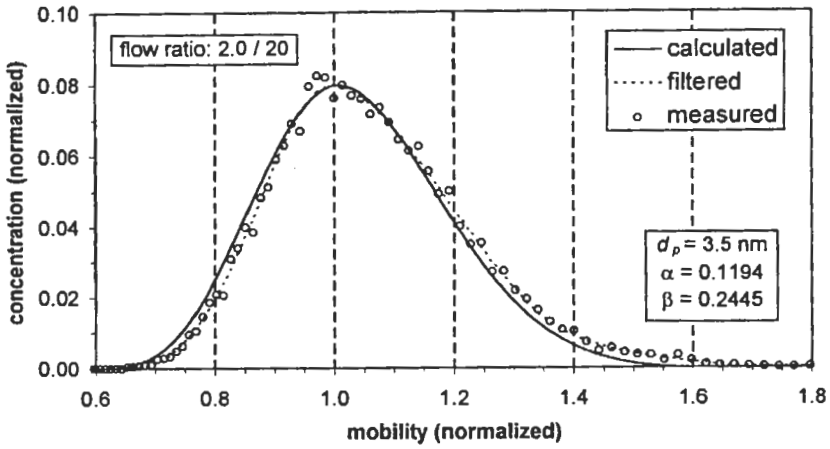

(c)

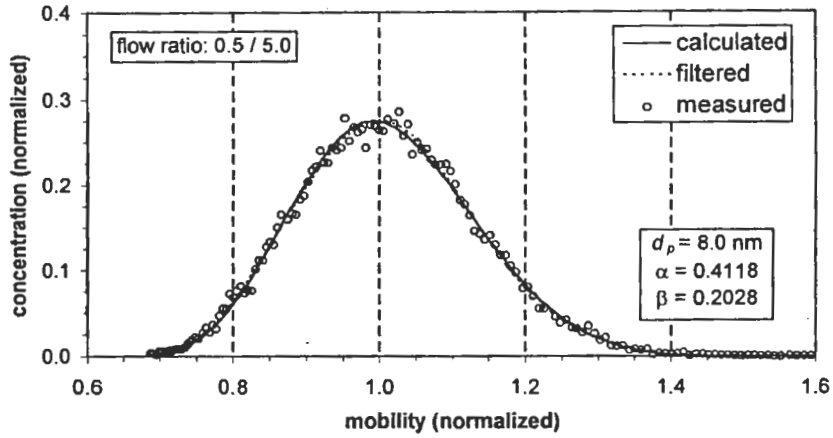

(d)

FIGURE 2b. (continued)

their position in the setup and by repeating the measurements. In all cases, the difference between the two measurements was within the expected error range. The estimated errors for α and β are smaller than $\pm 10\%$ and result primarily from flow rate uncertainties of the DMA.

With decreasing particle size ($d_p < 8$ nm), an additional error arises: Figure 2a–d shows the tandem DMA response comparing experimental to theoretically retrieved scans. Data for the smallest particle diameters $d_p = 10$, 6.0, and 3.5 nm (Vienna short) and for $d_p = 8.0$ nm (CIT radial) are presented. It can be seen that for $d_p = 10$ and 8.0 nm, experimental and calculated responses match very well. This also holds for all larger particle sizes (for these two particular DMAs). For $d_p = 6$ and 3.5 nm, deviations occur with respect to the slopes and the right-hand tail of the bell-shaped curves because the parameters α and β begin to change significantly during the scan procedure (rendering the curve more asym-

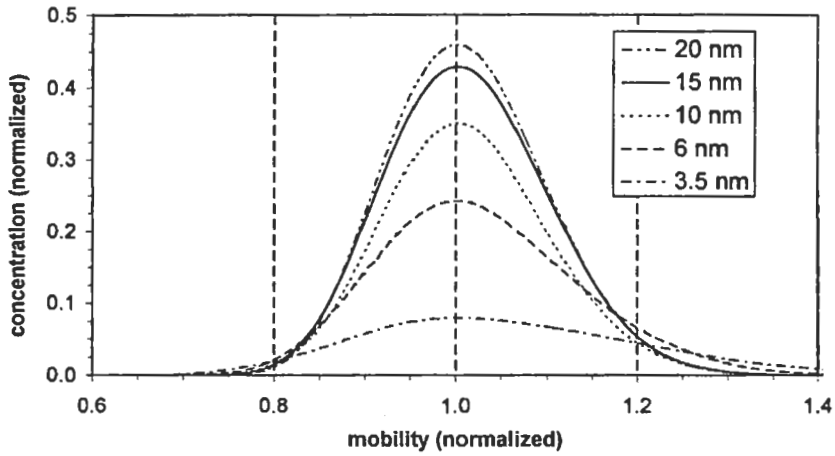

FIGURE 3. Degradation of the tandem DMA response (Vienna short) for decreasing particle size.

metric), which is the result of a strong variation of the particle diffusion coefficient with particle size. As a consequence, calculated values of α and β become less accurate. In a further study, it will be shown (Stratmann, 1997) that the deviations are not due to the use of a triangular shape for the transfer function in the deconvolution algorithm.

3. RESULTS AND DISCUSSION

Figure 3 illustrates the tandem DMA response (experimental data, filtered) for particle sizes from 20 down to 3.5 nm. Toward smaller particles, the curves flatten and become more asymmetric (see preceding text). In Fig. 3, only data from the Vienna short DMA are presented, but similar observations were made for all DMAs.

The experimentally determined parameters of the DMA transfer function (mean half-width β, height α, and area A) are plotted as a function of particle diameter d_p [nm] in Fig. 4a–e, for each DMA type separately. For easy application, exponential curves were fitted to all data. See Table 2 for the resulting fit coefficients. Some of these coefficients have concrete meanings, such as asymptotic values (a_0, b_0, A_0); others (d_m, d_0) represent the particle diameter at which the exponential function drops to 63.2% of its maximum value.

As a common observation for all five DMAs, all curves level off toward larger particle diameters. Below a certain diameter that is characteristic for each DMA, the height α of the transfer function decreases significantly with particle size, whereas its half-width β increases. The area A, as the product of both, also drops toward lower particle diameter. This latter observation agrees with previous measurements and can be explained by particle losses due to Brownian diffusion (cf. Zhang et al., 1995; Fissan et al., 1996). The theoretical values of the parameters of the transfer function (in the absence of diffusion) are $\alpha = 1.0$, $\beta = 0.1$, and $A = 0.1$ (except for the TSI long: $\alpha = 1.0$, $\beta = 0.2$, and $A = 0.2$). For the transfer function area A, all curves reach the correct limit for large particles indicating neglectable transport losses for such particles. The limiting values of α and β, however, are not reached for the CIT and all Vienna types. This may be indicative of flow disturbances in the classification section of these instruments.

When comparing the two DMAs used for the size range $d_p > 15$ nm, the Vienna medium (c) and the TSI long (d), one can see that they exhibit a similar behavior

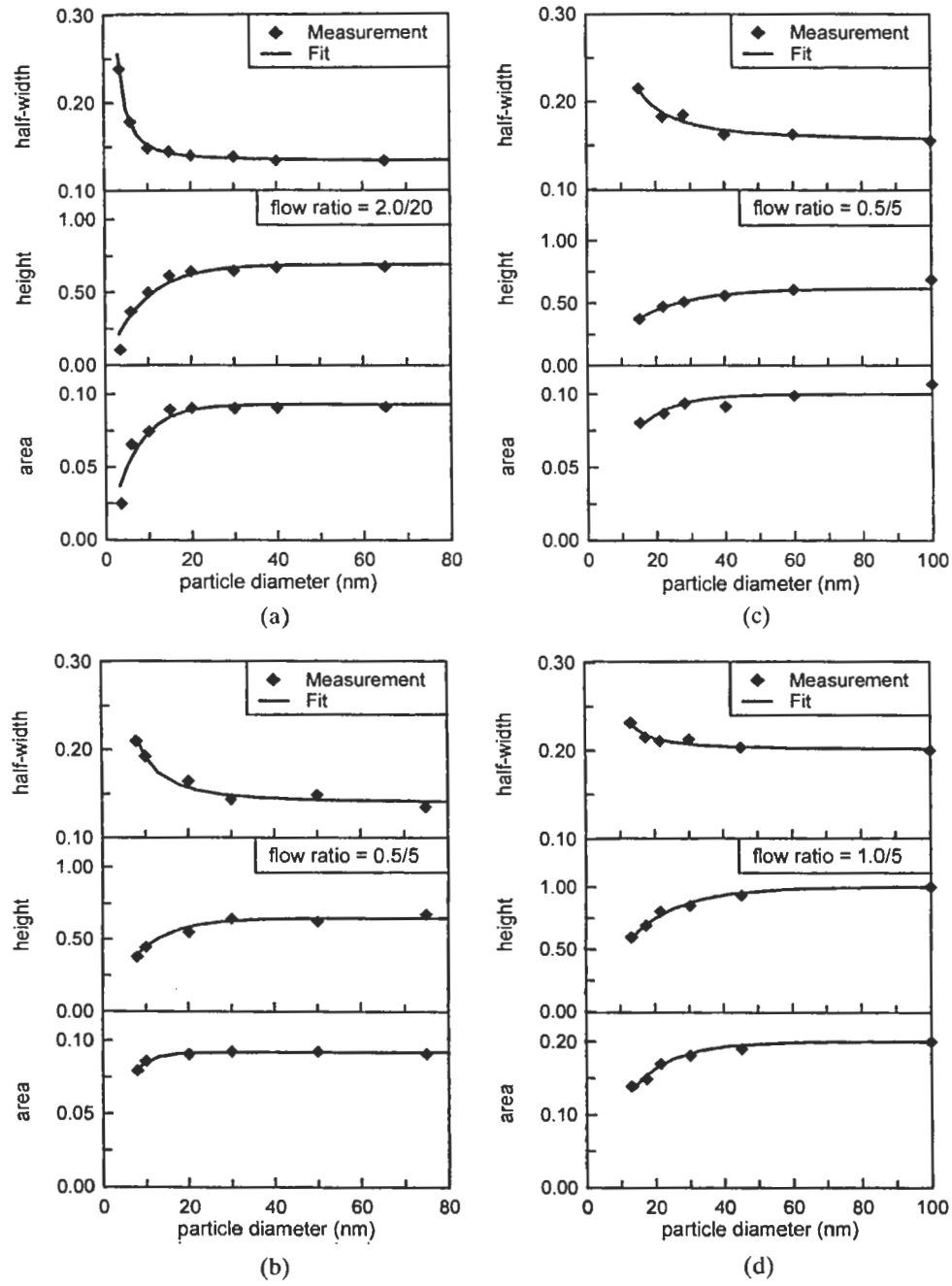

FIGURE 4. (a) Vienna short DMA, experimentally determined parameters of the DMA transfer functions. (b) CIT radial, experimentally determined parameters of the DMA transfer function. (c) Vienna medium DMA, experimentally determined parameters of the DMA transfer function. (d) TSI long, experimentally determined parameters of the DMA transfer function. (e) Vienna long DMA, experimentally determined parameters of the DMA transfer function.

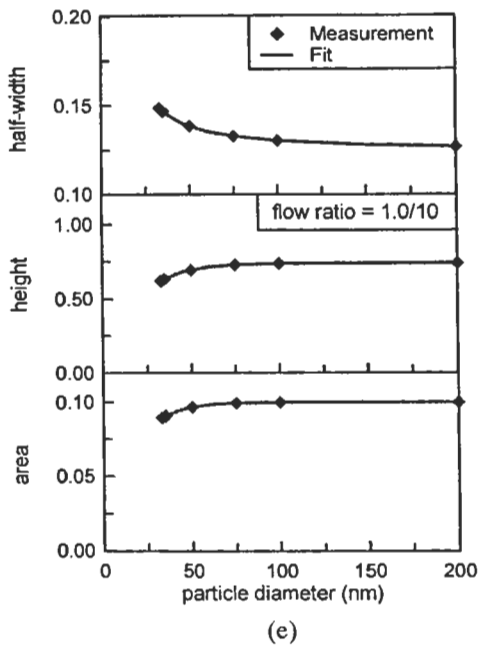

(e)

FIGURE 4. continued

apart from the fact that the ordinate scale of β and A is compressed by a factor of 2 for the TSI due to its different flow ratio. Two DMAs are suitable for measuring ultrafine particles: the Vienna short (a) and the CIT radial (b). The CIT features a larger transfer function area and thus a better particle transmission efficiency below 20 nm. On the other hand, the half-width β of the CIT rises faster when going toward smaller particles, implying that its particle size resolution is lower than that of the Vienna short below 20 nm. The lower resolution of the CIT might be explained by the different particle residence time. In the CIT, this residence time is four times longer than in the Vienna short (due to different flows), and thus particle diffusion is enhanced. Finally, the Vienna long DMA (e), reveals the lowest transmission (highest d_0) in the ultrafine region of the five DMA types studied, due to the longest residence time of particles inside the device.

After all, it is essential to keep in mind that the flow rates of all DMAs are critical in determining the DMA performance. The values used in this experiment were chosen to satisfy different sampling criteria (ACE1, ACE2). Consequently, a direct comparison of the different DMA types is only suitable to a limited extent.

4. CONCLUSION

The transfer functions for five different DMA types were determined experimentally over a wide diameter range. All DMAs tested share the feature that the height of the transfer function decreases toward lower particle size, whereas its width increases. This result is consistent with diffusional broadening of ultrafine particle trajectories (Kousaka et al., 1985). In addition,

TABLE 2. Coefficients of the Curves Fitted to the Experimentally Determined Transfer Function Parameters

Formula Expression Used for Fit	Half-width $\beta(d_p)$ $b_0+b_1\cdot d_p^{-q}$			Height $\alpha(d_p)$ $a_0\cdot(1.0-\exp(-d_p/d_m))$		Area $A(d_p)$ $A_0\cdot(1.0-\exp(-d_p/d_0))$	
Fit Parameters	b_0	b_1	q	a_0	d_m	A_0	d_0
(a) Vienna Type (short)	0.134	0.852	1.672	0.691	8.653	0.093	6.311
(b) CIT Radial	0.139	2.06	1.585	0.648	8.476	0.092	3.902
(c) Vienna Type (medium)	0.155	3.90	1.540	0.618	15.83	0.10[a]	10.10
(d) TSI Long	0.201	4.26	1.935	1.00[a]	14.42	0.20[a]	11.84
(e) Vienna Type (long)	0.125	2.28	1.304	0.740	18.27	0.10[a]	14.68

[a] Parameter was held fixed at this value during fitting.

the area of the transfer function drops toward lower particle size. This feature is the result of particle losses due to Brownian diffusion. The rate with which the transfer function area changes, however, is different for all DMA types.

L. M. R. appreciates the support of the National Science Foundation (grant ATM-9307603) and the Office of Naval Research for participation in ACE1 activities.

References

Fissan, H., Hummes, D., Stratmann, F., Buescher, P., and Neumann, S. (1996). Experimental Comparison of Four Differential Mobility Analyzers for Nanometer Aerosol Measurements, *Aerosol Sci. Technol.* 24:1–13.

Kousaka, Y., Okuyama, K., and Adachi, M. (1985). Determination of Particle Size Distribution of Ultra-fine Aerosols Using a Differential Mobility Analyzer, *Aerosol Sci. Technol.* 4:209–225.

Scheibel, H. G. and Porstendörfer, J. (1983). *J. Aerosol Sci.* 14:113–126.

Stolzenburg, M. R. (1988). An Ultrafine Aerosol Size Distribution Measuring System. Ph.D. thesis, University of Minnesota.

Stratmann, F., Kauffeldt, T., and Henning, S. (1997). Unpublished.

Stratmann, F., Kauffeldt, T., Hummes, D., and Fissan, H. (1996). Differential Electrical Mobility Analysis: A Theoretical Study, *Aerosol Sci. Technol.*, to appear.

Wang, S. C. and Flagan, R. C. (1990). Scanning Electrical Mobility Spectrometer, *Aerosol Sci. Technol.* 13:230–240.

Winkelmayr, W., Reischl, G. P., Linde, A. O., and Berner, A. (1991). A New Electromobility Spectrometer for the Measurement of Aerosol Size Distributions in the Size Range from 1 to 1000 NM, *J. Aerosol Sci.* 22:289–296.

Zhang, S. H., Akutsu, Y., Russell, L. M., Flagan, R. C., and Seinfeld, J. H. (1995). Radial Differential Mobility Analyzer, *Aerosol Sci. Technol.* 23:357–372.

Received 4 April 1996; accepted 16 December 1996